JACS
JOURNAL OF THE AMERICAN CHEMICAL SOCIETY
Communication
Cite This: J. Am. Chem. Soc. XXXX, XXX, XXX−XXX
pubs.acs.org/JACS

Multiple Bonding in Lanthanides and Actinides: Direct Comparison of Covalency in Thorium(IV)- and Cerium(IV)-Imido Complexes

Thibault Cheisson,[†,§] Kyle D. Kersey,[†,§] Nolwenn Mahieu,[†,‡,§] Alex McSkimming,[†] Michael R. Gau,[†] Patrick J. Carroll,[†] and Eric J. Schelter*[,†]

[†]P. Roy and Diana T. Vagelos Laboratories, Department of Chemistry, University of Pennsylvania, 231 South 34th Street, Philadelphia, Pennsylvania 19104, United States

[‡]Département de Chimie, ENS Paris-Saclay, Université Paris-Saclay, 94235 Cachan, France

Supporting Information

ABSTRACT: A series of thorium(IV)-imido complexes was synthesized and characterized. Extensive experimental and computational comparisons with the isostructural cerium(IV)-imido complexes revealed a notably more covalent bonding arrangement for the Ce═N bond compared with the more ionic Th═N bond. The thorium-imido moieties were observed to be 3 orders of magnitude more basic than their cerium congeners. More generally, these results provide unique experimental evidence for the larger covalent character of $4f^0 5d^0$ Ce(IV) multiple bonds compared to its $5f^0 6d^0$ Th(IV) actinide congener.

Chemical bonding in lanthanide and actinide compounds pushes our understanding and description of metal−ligand interactions. Fundamental understanding of these metal−ligand bonds redefines comprehension of the elements, even 150 years after the disclosure of the periodic trends, and contributes to new applications in reactivity.[1] This knowledge also has important implications for the treatment of the spent nuclear fuel or the purification of medical radioisotopes.[2] Metal−ligand multiple bonds are especially well-suited to experimentally interrogate fundamental differences between lanthanides and actinides.[3] While such chemistry has been extensively developed with early actinides,[3a,b,4] there have been very limited examples of such compounds with lanthanides.[5] In recent years, our group and others have developed the chemistry of Ce(IV)−ligand multiple bonds.[6] More is known for Th(IV),[3b,4a,7] the actinide analogue of Ce(IV); however, direct experimental comparison between these two elements is scarce.[3g−k,6h] Following the isolation of Ce(IV)-imido complexes employing the $TriNOx^{3-}$ framework (tris(2-*tert*-butylhydroxylaminato)benzylamine) by our group, we set out to contrast these compounds with isostructural Th(IV)-imido complexes. Structural, computational, and reactivity studies revealed marked differences between the two elements and, notably, highlighted that the extent of metal−ligand covalent bonding was larger for Ce(IV)- than Th(IV)-nitrogen double bonds as exemplified by multiple analyses, including thermodynamic metrics such as the acidity constant of these species.

Alkylation of [ThCl(TriNOx)] (**1**) with $LiCH_2(SiMe_3)$ afforded $[Th(CH_2SiMe_3)(TriNOx)]$ (**2**) that was employed to generate the anilide complex $[Th(NHAr^F)(TriNOx)]$ (**3**) by protonolysis with 3,5-bis(trifluoromethyl)aniline (Ar^FNH_2, Scheme 1).

Scheme 1. Syntheses of the new Th(IV)-Imido Complexes

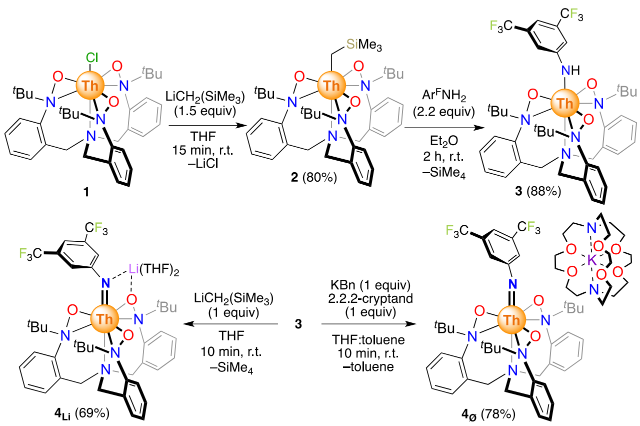

All complexes were characterized by multinuclear NMR spectroscopy, elemental analysis, and X-ray crystallography (Figures S1−S20). By analogy with our work on the synthesis of the Ce(IV)-imido complexes of general formulas $[M(L)_x]$-$[Ce{=}NAr^F(TriNOx)]$ with M = alkali metals and L = solvent or 2.2.2-cryptand,[6e,f] we first examined the deprotonenation of **3** using $MN(SiMe_3)_2$ with M = Li, K. Surprisingly, no reaction was observed. Stronger bases were required to induce the deprotonation of **3**: addition of $LiCH_2SiMe_3$ afforded a yellow solution of $\mathbf{4_{Li}}$ that was isolated in 69% yield (Scheme 1). Infrared spectroscopy and ^1H NMR demonstrated the loss of the NH moieties, while the resonances associated with the *ortho-* and *para-*position of the Ar^F group were largely shielded in comparison with **3** ($\Delta\delta$ = 0.47 and 0.43 ppm respectively, THF-d_8) as similarly observed in related cerium(IV) complexes.[6f,g] Layering a THF solution of $\mathbf{4_{Li}}$ with *n*-pentane at −20 °C afforded single crystals that established the formation of a lithium-capped thorium-imido complex typical of the $TriNOx^{3-}$ framework (Figure 1A).[6e−g]

Received: April 15, 2019

DOI: 10.1021/jacs.9b04061
J. Am. Chem. Soc. XXXX, XXX, XXX−XXX

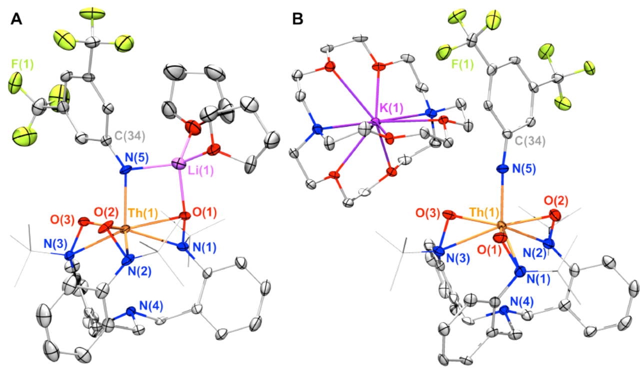

Figure 1. Thermal ellipsoid plots of 4_{Li} (A) and $4_ø$ (B) at 50% probability.

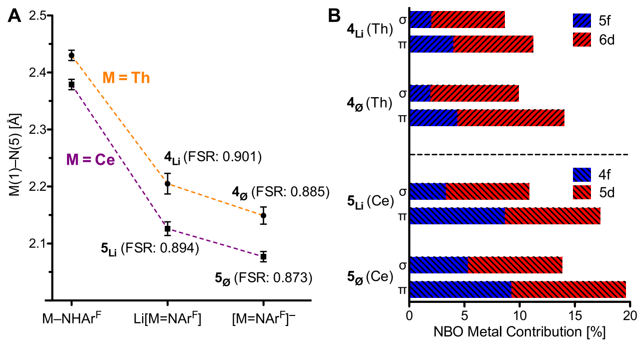

Figure 2. (A) Comparison of the M(1)−N(5) bond lengths in the anilide and imido complexes and derived formal shortness ratios (FSR). (B) Metal contributions to the σ- and π-bonding interactions and the relative contributions of the f and d orbitals as calculated by DFT/NBO 6.0.

In order to limit the influence of the ancillary lithium cation in the bonding scheme of the thorium-imido, we also pursued the synthesis of an uncapped thorium-imido complex. Treating a mixture of **3** and 2.2.2-cryptand with a THF solution of potassium benzyl afforded a vibrant yellow solution. A ^{1}H NMR spectrum showed an enhanced shielding of the *ortho*- and *para*-protons of the Ar^F moieties ($\Delta\delta$ = 0.90 and 0.79 ppm, respectively) in comparison with **3**. UV−visible spectroscopy demonstrated a broad absorption band centered at 420 nm (ε = 1540 M^{-1} cm^{-1}) assigned as a ligand-to-ligand charge transfer by TD-DFT calculations (Figures S43−S45).[8] This CT band was red-shifted in comparison with $\mathbf{4}_{Li}$ (Figure S21) prompting us to conclude the formation of the terminal imido complex $\mathbf{4}_ø$ (Scheme 1). Indeed, X-ray diffraction studies confirmed the sequestration of the potassium countercation and the presence of a bent terminal thorium-imido fragment (Th(1)−N(5)−C(34) 160.0(5)°, Figure 1B). $\mathbf{4}_{Li}$ and $\mathbf{4}_ø$ contribute to the relatively short list of previously characterized Th(IV)-imido complexes.[9] Most importantly **3**, $\mathbf{4}_{Li}$, and $\mathbf{4}_ø$ constitute nearly isostructural thorium-analogues of the previously structurally characterized Ce(IV)-anilide [Ce(NHAr^F)(TriNOx)] ($\mathbf{3}_{Ce}$) and Ce(IV)-imido complexes [Li(THF)(OEt$_2$)][Ce=NAr^F(TriNOx)] ($\mathbf{5}_{Li}$), and [Cs(2.2.2-cryptand)][Ce=NAr^F(TriNOx)] ($\mathbf{5}_ø$) respectively,[6e,f] creating a unique situation for the direct comparison of these structures. Mirroring the trend observed in the cerium(IV) series, the Th(1)−N(5) bond lengths decreased from 2.429(2) Å in **3** to 2.205(6) Å in the Li-capped imido $\mathbf{4}_{Li}$ to 2.149(5) Å for the terminal complex $\mathbf{4}_ø$ (Figure 2A). These Th=N bonds were in the longer end of the range for other reported Th-imido complexes (mean 2.10(5) Å),[9] likely caused by the electron-withdrawing CF$_3$ substituents.

When compared with the cerium analogues,[6f] the M(1)−N(5) distances were consistently longer in the thorium complexes (M = Ce, Th). This difference is primarily explained by the larger ionic radius of Th^{IV} (0.94 Å, CN 6) compared to Ce^{IV} (0.87 Å, CN 6).[10] However, the bond-shortening was more pronounced in the cerium-imido complexes as demonstrated by the smaller formal shortness ratios (Figure 2A). In order to explore differences in the bonding between these isostructural lanthanide- and actinide-imido complexes, we turned to computational analyses as previously performed for the cerium complexes. The Kohn−Sham frontier orbitals of the DFT-optimized structures of $\mathbf{4}_{Li}$ and $\mathbf{4}_ø$ demonstrated a clear interaction of π-symmetry between the imido N atom and the Th center, reminiscent to the bonding scheme of the cerium(IV) analogues. To understand the relative contribution of Ce and Th in the bonding of these molecules, a natural bond orbital (NBO) analysis was performed.[11] Again similar to our previous results,[6f,g] two NBO bonding interactions of respective σ- and π-symmetry were observed between the N and Th atoms (Figures S36−S37). These interactions were largely N-polarized but presented some Th character (9−14%). When compared with the results obtained for the corresponding Ce complexes $\mathbf{5}_{Li}$ and $\mathbf{5}_ø$,[6f] the NBO cerium contribution was superior (11 to 20%, Figure 2B). Therefore, suggesting a more ionic bonding situation for the thorium-imido complexes $\mathbf{4}_{Li}$ and $\mathbf{4}_ø$ than the cerium congeners $\mathbf{5}_{Li}$ and $\mathbf{5}_ø$. Apart from the different NBO metal contributions, the relative involvement of the 4f/5d (for Ce) and 5f/6d (for Th) orbitals in the bonding interactions were also different. The 6d orbitals of the Th centers were primarily involved in the bonding, while a more split situation was observed for Ce (Figure 2B) in agreement with other reports.[3h,j,6c] This observation can be rationalized by the characteristic of the Th(IV) cation for which the 6d shells are usually the valence orbitals, unlike the later actinides or the trivalent lanthanides.[12]

Taken together, the aforementioned structural and computational results suggested that thorium-imido complexes in the TriNOx^{3-} framework present a more ionic bonding situation than their cerium congeners. In that context, the necessity of employing alkyl bases (LiCH$_2$SiMe$_3$, KBn) to generate $\mathbf{4}_{Li}$ and $\mathbf{4}_ø$—when bis(trimethylsilyl)amide bases were suitable to form $\mathbf{5}_{Li}$ and $\mathbf{5}_ø$—was noteworthy and prompted a more detailed determination of the pK_a of **3** and $\mathbf{3}_{Ce}$ (all in THF at 300 K). Initial bracketing allowed narrowing of the pK_a range to 27−33 for **3** and 22−28 for $\mathbf{3}_{Ce}$ (Figures S24−S27). ^{1}H NMR titration studies of $\mathbf{3}_{Ce}$ with increments of LiN(SiMe$_3$)$_2$ (pK_a(HN(SiMe$_3$)$_2$) = 25.8)[13] returned a value of 25.2(2) for $\mathbf{3}_{Ce}$. We also confirmed that an excess of HN(SiMe$_3$)$_2$ would only partially re-protonate $\mathbf{5}_{Li}$ (Figure S28). For Th, ^{1}H NMR titrations of $\mathbf{4}_{Li}$ with HN(SiMe$_3$)(^{i}Pr) (pK_a= 31.6)[13] returned an acidity constant of 28.6(3) for **3** (Tables S3 and S4). Similarly, we confirmed that HN(SiMe$_3$)$_2$ would quantitatively re-protonate $\mathbf{4}_{Li}$. These results experimentally demonstrated that the Th(IV)-imido fragments described here are more than 3 orders of magnitude more basic than their Ce(IV) counterparts (Figure 3), in accord with the structural data reported above.

Although both Th(IV)- and Ce(IV)-imido complexes would be considered as superbases,[15] the large decrease in the thermodynamic basicity of the Ce(IV)-imidos can be

DOI: 10.1021/jacs.9b04061
J. Am. Chem. Soc. XXXX, XXX, XXX−XXX

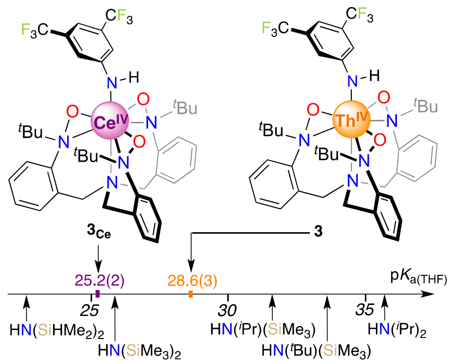

Figure 3. Experimentally determined pK_a of 3_{Ce} and **3** compared with common amide bases.[13,14]

(cautiously) compared to the results of Leung and Walter regarding terminal cerium- and thorium-oxo complexes.[6b,7a] Indeed, Th(IV)=O moieties were observed to possess an increased (kinetic) nucleophilic character compared to Ce(IV)=O bonds when reacted with ketones.

Although proton-coupled electron transfer was not noted in this work, the determination of the acidity constant of **3** and $\mathbf{3_{Ce}}$ allowed for the estimation of the N−H bond dissociation free energy (BDFE) of the putative reduced anilide complexes $\mathbf{3}^-$ and $\mathbf{3_{Ce}}^-$. We previously reported a quasi-reversible $Ce^{IV/III}$ redox couple for $\mathbf{5_{Li}}$ at −1.39 V vs $Fc^{+/0}$, predicting a BDFE(N−H) ≈ 68 kcal mol^{-1} in $\mathbf{3_{Ce}}^-$.[16] On the other hand, no metal- or ligand-based reduction events were observed in the cyclic voltammogram of $\mathbf{4_{Li}}$ (Figure S23). This suggests that a hypothetical complex $\mathbf{3}^-$ would present an extremely weak anilide N−H bond with a BDFE(N−H) < 32 kcal mol^{-1}.

After isolating a series of isostructural Th(IV)- and Ce(IV)-imido complexes and establishing their diverging thermodynamic properties, we were interested in exploring the possibility of transferring the imido moieties from one metallic center to the other. To that end, we synthesized a "naked" Ce(IV) complex $[Ce^{IV}(THF)(TriNOx)][BAr^F_4]$ ($\mathbf{6_{Ce}}$) able to accept the imido moiety from $\mathbf{4_{Li}}$ or $\mathbf{4_ø}$ to hypothetically form $\mathbf{5_{Li}}$ or $\mathbf{5_ø}$.[17] The addition of a dark THF-d_8 solution of $\mathbf{6_{Ce}}$ to a yellow solution of $\mathbf{4_ø}$ resulted instantly in a color change to a brown mixture, different from the expected intense purple color of $\mathbf{5_ø}$. The presence of well-known paramagnetic resonances in the ^{1}H NMR spectrum of the mixture were in agreement with the formation of the reduced Ce^{III} compound $[Ce^{III}(THF)(TriNOx)]$ (**7**).[17] Regarding the Th species, a product was formed whose ^{1}H NMR spectrum overlaid perfectly with the previously characterized anilide complex **3** (Figures S29−S32). The remaining signals in ^{1}H, ^{19}F, and ^{11}B NMR were in accord with the side production of an equivalent of $[K(2.2.2\text{-cryptand})][BAr^F_4]$ (Scheme 2).

Analysis of the reaction ^{1}H NMR spectrum revealed a lower than expected integration for the anilide proton (~30% of the

Scheme 2. Reaction of $\mathbf{4_ø}$ and $\mathbf{6_{Ce}}$ To Form 3-d_1 and 7

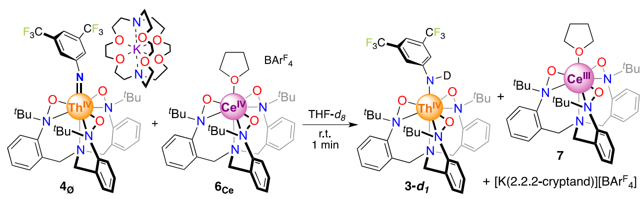

expected value). ^{2}H NMR spectroscopy revealed an incorporation of deuterium at the anilide position (Figure S35) demonstrating the formation of **3**-d_1 as the actual reaction product. The reaction was repeated in toluene-d_8 or starting from $\mathbf{4_{Li}}$, returning comparable results. The reaction was also conducted in solvent more resistant to H atom abstraction, 1,2-difluorobenzene,[18] without significantly altering the rate nor the outcome, probably suggesting that the bound THF molecule in $\mathbf{6_{Ce}}$ acts as the major $H^•$ source. These data point toward a radical mechanism to account for the observed reactivity. In turn, a plausible pathway would be an initial formation of bridged $Ce(IV)−NAr^F−Th(IV)$ intermediate leading to the homolytic cleavage of the Ce(IV)−N bond to form the reduced Ce(III) and a highly reactive Th(IV)-iminyl complex capable of $H^•$ abstraction. To evaluate that hypothesis, we turned to DFT calculations (Figure 4).

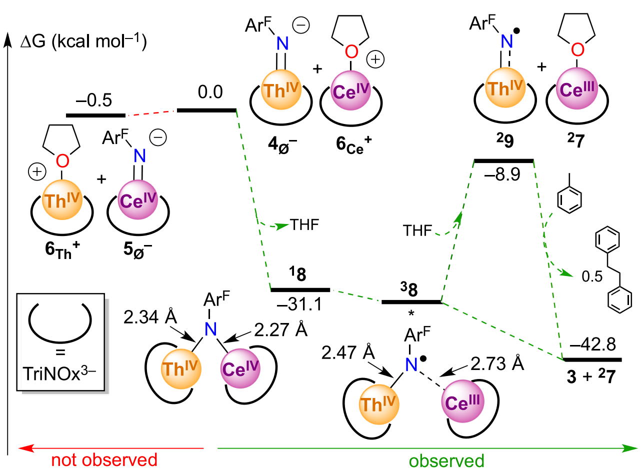

Figure 4. DFT-calculated reaction coordinates for the formation of **3** and **7**. *The energy of ^{3}**8** was not obtained.

We first evaluated the energies of $\mathbf{4_ø}^-$+ $\mathbf{6_{Ce}}^+$ and $\mathbf{5_ø}^-$+ $\mathbf{6_{Th}}^+$ revealing a nearly thermoneutral hypothetical exchange reaction. The formation of the postulated closed-shell bridging imido (^{1}**8**, Figure S38−S40) was found to be strongly downhill (−31.1 kcal mol^{-1}). Changing the multiplicity of ^{1}**8** to a triplet allowed for the pre-optimization of ^{3}**8**; however, due to computational limitation, we were not able to fully converge this intermediate and determine its energy (Figure S41). From the latter intermediate, the combination of the postulated N-centered Th(IV)-iminyl radical ^{2}**9** (Figure S42) and the Ce(III) complex ^{2}**7** was located −8.9 kcal mol^{-1} below the starting materials but about 22 kcal mol^{-1} above the bridging imido ^{1}**8**. The subsequent $H^•$ abstraction was modeled for the reaction of ^{2}**9** with toluene to form **3** and bibenzyl, revealing an overall exergonic process by ~43 kcal mol^{-1}. This calculated profile is in good agreement with our experimental observations of an instantaneous reaction at room temperature; however, the relatively high energy of ^{2}**9** + ^{2}**7** compared with the bridging species could suggest that the $H^•$ abstraction may happen directly from ^{3}**8**. We propose that the driving force for the homolytic rupture of the Ce−N bond resides in the formation of a long and distorted Ce−N interaction that limits the covalent character and therefore facilitates the reduction event.[19]

In summary, we report the synthesis and characterization of a series of Th(IV)-imido complexes. These compounds were

DOI: 10.1021/jacs.9b04061
J. Am. Chem. Soc. XXXX, XXX, XXX−XXX

structural analogues of previously isolated Ce(IV)-imido complexes and allowed for a comparison of this bonding motif between a lanthanide and an actinide for the first time. Structural, computational, and thermodynamic data support a more ionic fragment in the case of the thorium, posing the question of the amount of covalent character encountered in these Ce(IV)-imido complexes. It is generally accepted that the actinides are more covalent than the lanthanides. These results demonstrate that Ce(IV) can display an unusually large amount of covalent character that is notably more important than in early actinides such as Th(IV).[3h,6c,h] In that regard, the difference of more than 3 pK_a units between the Th(IV)- and Ce(IV)-anilides is a unique experimental evidence for this trend. Studies are underway in our laboratory to explore the reactivity and the unusual electronic structure of these complexes.

■ ASSOCIATED CONTENT

Supporting Information

The Supporting Information is available free of charge on the ACS Publications website at DOI: 10.1021/jacs.9b04061.

Experimental procedures, spectroscopic data, and computational details (PDF)

Crystallographic data for **1**, **2**, **3**, $\mathbf{4_{Li}}$, $\mathbf{4_{\o}}$, and $\mathbf{6_{Th}}$ (CIF)

Cartesian coordinates for DFT-optimized structures (XYZ)

■ AUTHOR INFORMATION

Corresponding Author

*schelter@sas.upenn.edu

ORCID

Thibault Cheisson: 0000-0003-4359-5115

Nolwenn Mahieu: 0000-0003-2280-3616

Michael R. Gau: 0000-0002-4790-6980

Eric J. Schelter: 0000-0002-8143-6206

Author Contributions

§T.C., K.D.K., and N.M. contributed equally.

Notes

The authors declare no competing financial interest.

■ ACKNOWLEDGMENTS

The authors gratefully acknowledge the U.S. National Science Foundation (CHE-1664928) for primary support. We also thank the University of Pennsylvania for support of this work. T.C. and A.M. acknowledge the Center for Actinide Science and Technology (CAST), an Energy Frontier Research Center (EFRC) funded by the U.S. Department of Energy, Office of Science, Basic Energy Sciences, under Award Number DE-SC0016568 for support. This work used the Extreme Science and Engineering Discovery Environment (XSEDE), which is supported by NSF (ACI-1548562). K.D.K. acknowledges the Vagelos Integrated Program in Energy Research (VIPER) of the University of Pennsylvania for a summer research undergraduate fellowship.

■ REFERENCES

(1) (a) Cheisson, T.; Schelter, E. J. Rare Earths Elements: Mendeleev's Bane, Modern Marvels. *Science* **2019**, *363*, 489−493. (b) Cary, S. K.; Vasiliu, M.; Baumbach, R. E.; Stritzinger, J. T.; Green, T. D.; Diefenbach, K.; Cross, J. N.; Knappenberger, K. L.; Liu, G.; Silver, M. A.; DePrince, A. E.; Polinski, M. J.; Van Cleve, S. M.; House, J. H.; Kikugawa, N.; Gallagher, A.; Arico, A. A.; Dixon, D. A.; Albrecht-Schmitt, T. E. Emergence of californium as the second transitional element in the actinide series. *Nat. Commun.* **2015**, *6*, 6827. (c) Silver, M. A.; Cary, S. K.; Garza, A. J.; Baumbach, R. E.; Arico, A. A.; Galmin, G. A.; Chen, K.-W.; Johnson, J. A.; Wang, J. C.; Clark, R. J.; Chemey, A.; Eaton, T. M.; Marsh, M. L.; Seidler, K.; Galley, S. S.; van de Burgt, L.; Gray, A. L.; Hobart, D. E.; Hanson, K.; Van Cleve, S. M.; Gendron, F.; Autschbach, J.; Scuseria, G. E.; Maron, L.; Speldrich, M.; Kögerler, P.; Celis-Barros, C.; Páez-Hernández, D.; Arratia-Pérez, R.; Ruf, M.; Albrecht-Schmitt, T. E. Electronic Structure and Properties of Berkelium Iodates. *J. Am. Chem. Soc.* **2017**, *139*, 13361−13375. (d) Xémard, M.; Zimmer, S.; Cordier, M.; Goudy, V.; Ricard, L.; Clavaguéra, C.; Nocton, G. Lanthanidocenes: Synthesis, Structure, and Bonding of Linear Sandwich Complexes of Lanthanides. *J. Am. Chem. Soc.* **2018**, *140*, 14433−14439. (e) Kelley, M. P.; Bessen, N. P.; Su, J.; Urban, M.; Sinkov, S. I.; Lumetta, G. J.; Batista, E. R.; Yang, P.; Shafer, J. C. Revisiting complexation thermodynamics of transplutonium elements up to einsteinium. *Chem. Commun.* **2018**, *54*, 10578−10581. (f) Walter, M. D.; Booth, C. H.; Lukens, W. W.; Andersen, R. A. Cerocene Revisited: The Electronic Structure of and Interconversion Between $Ce_2(C_8H_8)_3$ and $Ce(C_8H_8)_2$. *Organometallics* **2009**, *28*, 698−707. (g) Galley, S. S.; Pattenaude, S. A.; Gaggioli, C. A.; Qiao, Y.; Sperling, J. M.; Zeller, M.; Pakhira, S.; Mendoza-Cortes, J. L.; Schelter, E. J.; Albrecht-Schmitt, T. E.; Gagliardi, L.; Bart, S. C. Synthesis and Characterization of Tris-chelate Complexes for Understanding f-Orbital Bonding in Later Actinides. *J. Am. Chem. Soc.* **2019**, *141*, 2356−2366. (h) Coughlin, E. J.; Qiao, Y.; Lapsheva, E.; Zeller, M.; Schelter, E. J.; Bart, S. C. Uranyl Functionalization Mediated by Redox-Active Ligands: Generation of O−C Bonds via Acylation. *J. Am. Chem. Soc.* **2019**, *141*, 1016−1026. (i) Hayton, T. W.; Boncella, J. M.; Scott, B. L.; Palmer, P. D.; Batista, E. R.; Hay, P. J. Synthesis of Imido Analogs of the Uranyl Ion. *Science* **2005**, *310*, 1941. (j) Billow, B. S.; Livesay, B. N.; Mokhtarzadeh, C. C.; McCracken, J.; Shores, M. P.; Boncella, J. M.; Odom, A. L. Synthesis and Characterization of a Neutral U(II) Arene Sandwich Complex. *J. Am. Chem. Soc.* **2018**, *140*, 17369−17373. (k) Qiao, Y.; Schelter, E. J. Lanthanide Photocatalysis. *Acc. Chem. Res.* **2018**, *51*, 2926−2936.

(2) (a) Ferrier, M. G.; Stein, B. W.; Bone, S. E.; Cary, S. K.; Ditter, A. S.; Kozimor, S. A.; Lezama Pacheco, J. S.; Mocko, V.; Seidler, G. T. The coordination chemistry of Cm^{III}, Am^{III}, and Ac^{III} in nitrate solutions: an actinide L_3-edge EXAFS study. *Chem. Sci.* **2018**, *9*, 7078−7090. (b) Bell, N. L.; Shaw, B.; Arnold, P. L.; Love, J. B. Uranyl to Uranium(IV) Conversion through Manipulation of Axial and Equatorial Ligands. *J. Am. Chem. Soc.* **2018**, *140*, 3378−3384. (c) Captain, I.; Deblonde, G. J. P.; Rupert, P. B.; An, D. D.; Illy, M.-C.; Rostan, E.; Ralston, C. Y.; Strong, R. K.; Abergel, R. J. Engineered Recognition of Tetravalent Zirconium and Thorium by Chelator−Protein Systems: Toward Flexible Radiotherapy and Imaging Platforms. *Inorg. Chem.* **2016**, *55*, 11930−11936. (d) Mastren, T.; Radchenko, V.; Owens, A.; Copping, R.; Boll, R.; Griswold, J. R.; Mirzadeh, S.; Wyant, L. E.; Brugh, M.; Engle, J. W.; Nortier, F. M.; Birnbaum, E. R.; John, K. D.; Fassbender, M. E. Simultaneous Separation of Actinium and Radium Isotopes from a Proton Irradiated Thorium Matrix. *Sci. Rep.* **2017**, *7*, 8216. (e) Mishiro, K.; Hanaoka, H.; Yamaguchi, A.; Ogawa, K. Radiotheranostics with radiolanthanides: Design, development strategies, and medical applications. *Coord. Chem. Rev.* **2019**, *383*, 104−131.

(3) (a) Tatebe, C. J.; Gettys, K. E.; Bart, S. C. Reactivity of Actinide Imido Complexes. In *Handbook on the Physics and Chemistry of Rare Earths*; Bünzli, J.-C. G., Pecharsky, V. K., Eds.; Elsevier: Amsterdam, 2018; Vol. *54*, Chap. 303, pp 1−42. (b) Boreen, M. A.; Arnold, J., Multiple Bonding in Actinide Chemistry. In *Encyclopedia of Inorganic and Bioinorganic Chemistry*; Scott, R. A., Ed.; Wiley: Hoboken, 2018. DOI: 10.1002/9781119951438.eibc2535. (c) Minasian, S. G.; Batista, E. R.; Booth, C. H.; Clark, D. L.; Keith, J. M.; Kozimor, S. A.; Lukens, W. W.; Martin, R. L.; Shuh, D. K.; Stieber, S. C. E.; Tyliszczak, T.; Wen, X.-d. Quantitative Evidence for Lanthanide-Oxygen Orbital Mixing in CeO_2, PrO_2, and TbO_2. *J. Am. Chem. Soc.* **2017**, *139*,

18052−18064. (d) Neidig, M. L.; Clark, D. L.; Martin, R. L. Covalency in f-element complexes. *Coord. Chem. Rev.* **2013**, *257*, 394−406. (e) Löble, M. W.; Keith, J. M.; Altman, A. B.; Stieber, S. C. E.; Batista, E. R.; Boland, K. S.; Conradson, S. D.; Clark, D. L.; Lezama Pacheco, J.; Kozimor, S. A.; Martin, R. L.; Minasian, S. G.; Olson, A. C.; Scott, B. L.; Shuh, D. K.; Tyliszczak, T.; Wilkerson, M. P.; Zehnder, R. A. Covalency in Lanthanides. An X-ray Absorption Spectroscopy and Density Functional Theory Study of $LnCl_6^{x-}$ (x = 3, 2). *J. Am. Chem. Soc.* **2015**, *137*, 2506−2523. (f) Minasian, S. G.; Boland, K. S.; Feller, R. K.; Gaunt, A. J.; Kozimor, S. A.; May, I.; Reilly, S. D.; Scott, B. L.; Shuh, D. K. Synthesis and Structure of $(Ph_4P)_2MCl_6$ (M = Ti, Zr, Hf, Th, U, Np, Pu). *Inorg. Chem.* **2012**, *51*, 5728−5736. (g) Wu, Q.-Y.; Cheng, Z.-P.; Lan, J.-H.; Wang, C.-Z.; Chai, Z.-F.; Gibson, J. K.; Shi, W.-Q. Insight into the nature of M−C bonding in the lanthanide/actinide-biscarbene complexes: a theoretical perspective. *Dalton Trans.* **2018**, *47*, 12718−12725. (h) Berryman, V. E. J.; Whalley, Z. J.; Shephard, J. J.; Ochiai, T.; Price, A. N.; Arnold, P. L.; Parsons, S.; Kaltsoyannis, N. Computational analysis of M−O covalency in $M(OC_6H_5)_4$ (M = Ti, Zr, Hf, Ce, Th, U). *Dalton Trans.* **2019**, *48*, 2939−2947. (i) Cary, S. K.; Livshits, M.; Cross, J. N.; Ferrier, M. G.; Mocko, V.; Stein, B. W.; Kozimor, S. A.; Scott, B. L.; Rack, J. J. Advancing Understanding of the + 4 Metal Extractant Thenoyltrifluoroacetonate (TTA^-); Synthesis and Structure of $M^{IV}TTA_4$ (M^{IV} = Zr, Hf, Ce, Th, U, Np, Pu) and $M^{III}(TTA)_4^-$ (M^{III} = Ce, Nd, Sm, Yb). *Inorg. Chem.* **2018**, *57*, 3782−3797. (j) Lu, E.; Sajjad, S.; Berryman, V. E. J.; Wooles, A. J.; Kaltsoyannis, N.; Liddle, S. T. Emergence of the structure-directing role of f-orbital overlap-driven covalency. *Nat. Commun.* **2019**, *10*, 634. (k) Behrle, A. C.; Levin, J. R.; Kim, J. E.; Drewett, J. M.; Barnes, C. L.; Schelter, E. J.; Walensky, J. R. Stabilization of M^{IV} = Ti, Zr, Hf, Ce, and Th using a selenium bis(phenolate) ligand. *Dalton Trans* **2015**, *44*, 2693−2702.

(4) (a) Hayton, T. W. Recent developments in actinide−ligand multiple bonding. *Chem. Commun.* **2013**, *49*, 2956−2973. (b) Mullane, K. C.; Ryu, H.; Cheisson, T.; Grant, L. N.; Park, J. Y.; Manor, B. C.; Carroll, P. J.; Baik, M.-H.; Mindiola, D. J.; Schelter, E. J. C−H Bond Addition across a Transient Uranium−Nitrido Moiety and Formation of a Parent Uranium Imido Complex. *J. Am. Chem. Soc.* **2018**, *140*, 11335−11340. (c) Falcone, M.; Chatelain, L.; Scopelliti, R.; Živković, I.; Mazzanti, M. Nitrogen reduction and functionalization by a multimetallic uranium nitride complex. *Nature* **2017**, *547*, 332. (d) King, D. M.; Tuna, F.; McInnes, E. J. L.; McMaster, J.; Lewis, W.; Blake, A. J.; Liddle, S. T. Synthesis and Structure of a Terminal Uranium Nitride Complex. *Science* **2012**, *337*, 717.

(5) (a) Zhu, Q.; Zhu, J.; Zhu, C. Recent progress in the chemistry of lanthanide-ligand multiple bonds. *Tetrahedron Lett.* **2018**, *59*, 514−520. (b) Schädle, D.; Meermann-Zimmermann, M.; Schädle, C.; Maichle-Mössmer, C.; Anwander, R. Rare-Earth Metal Complexes with Terminal Imido Ligands. *Eur. J. Inorg. Chem.* **2015**, *2015*, 1334−1339. (c) Chan, H.-S.; Li, H.-W.; Xie, Z. Synthesis and structural characterization of imido-lanthanide complexes with a metal-nitrogen multiple bond. *Chem. Commun.* **2002**, 652−653.

(6) (a) So, Y.-M.; Wang, G.-C.; Li, Y.; Sung, H. H. Y.; Williams, I. D.; Lin, Z.; Leung, W.-H. A Tetravalent Cerium Complex Containing a Ce = O Bond. *Angew. Chem., Int. Ed.* **2014**, *53*, 1626−1629. (b) So, Y.-M.; Li, Y.; Au-Yeung, K.-C.; Wang, G.-C.; Wong, K.-L.; Sung, H. H. Y.; Arnold, P. L.; Williams, I. D.; Lin, Z.; Leung, W.-H. Probing the Reactivity of the Ce = O Multiple Bond in a Cerium(IV) Oxo Complex. *Inorg. Chem.* **2016**, *55*, 10003−10012. (c) Damon, P. L.; Wu, G.; Kaltsoyannis, N.; Hayton, T. W. Formation of a Ce(IV) Oxo Complex via Inner Sphere Nitrate Reduction. *J. Am. Chem. Soc.* **2016**, *138*, 12743−12746. (d) Assefa, M. K.; Wu, G.; Hayton, T. W. Synthesis of a terminal Ce(iv) oxo complex by photolysis of a Ce(iii) nitrate complex. *Chem. Sci.* **2017**, *8*, 7873−7878. (e) Solola, L. A.; Zabula, A. V.; Dorfner, W. L.; Manor, B. C.; Carroll, P. J.; Schelter, E. J. An Alkali Metal-Capped Cerium(IV) Imido Complex. *J. Am. Chem. Soc.* **2016**, *138*, 6928−6931. (f) Solola, L. A.; Zabula, A. V.; Dorfner, W. L.; Manor, B. C.; Carroll, P. J.; Schelter, E. J. Cerium(IV) Imido Complexes: Structural, Computational, and Reactivity Studies. *J. Am. Chem. Soc.* **2017**, *139*, 2435−2442. (g) Cheisson, T.; Solola, L. A.; Gau, M. R.; Carroll, P. J.; Schelter, E. J. Silyl Transfer Pathway to a Ce(IV) Imido Complex. *Organometallics* **2018**, *37*, 4332−4335. (h) Gregson, M.; Lu, E.; Tuna, F.; McInnes, E. J. L.; Hennig, C.; Scheinost, A. C.; McMaster, J.; Lewis, W.; Blake, A. J.; Kerridge, A.; Liddle, S. T. Emergence of comparable covalency in isostructural cerium(iv)− and uranium(iv)−carbon multiple bonds. *Chem. Sci.* **2016**, *7*, 3286−3297.

(7) (a) Ren, W.; Zi, G.; Fang, D.-C.; Walter, M. D. Thorium Oxo and Sulfido Metallocenes: Synthesis, Structure, Reactivity, and Computational Studies. *J. Am. Chem. Soc.* **2011**, *133*, 13183−13196. (b) Smiles, D. E.; Wu, G.; Hrobárik, P.; Hayton, T. W. Use of ^{77}Se and ^{125}Te NMR Spectroscopy to Probe Covalency of the Actinide-Chalcogen Bonding in $[Th(E_n)\{N(SiMe_3)_2\}_3]^-$ (E = Se, Te; n = 1, 2) and Their Oxo-Uranium(VI) Congeners. *J. Am. Chem. Soc.* **2016**, *138*, 814−825. (c) Vilanova, S. P.; Alayoglu, P.; Heidarian, M.; Huang, P.; Walensky, J. R. Metal−Ligand Multiple Bonding in Thorium Phosphorus and Thorium Arsenic Complexes. *Chem. - Eur. J.* **2017**, *23*, 16748−16752. (d) Rungthanaphatsophon, P.; Bathelier, A.; Castro, L.; Behrle, A. C.; Barnes, C. L.; Maron, L.; Walensky, J. R. Formation of Methane versus Benzene in the Reactions of $(C_5Me_5)_2Th(CH_3)_2$ with $[CH_3PPh_3]X$ (X = Cl, Br, I) Yielding Thorium-Carbene or Thorium-Ylide Complexes. *Angew. Chem., Int. Ed.* **2017**, *56*, 12925−12929. (e) Lu, E.; Lewis, W.; Blake, A. J.; Liddle, S. T. The Ketimide Ligand is Not Just an Inert Spectator: Heteroallene Insertion Reactivity of an Actinide−Ketimide Linkage in a Thorium Carbene Amide Ketimide Complex. *Angew. Chem., Int. Ed.* **2014**, *53*, 9356−9359. (f) Zhang, C.; Hou, G.; Zi, G.; Ding, W.; Walter, M. D. A Base-Free Terminal Actinide Phosphinidene Metallocene: Synthesis, Structure, Reactivity, and Computational Studies. *J. Am. Chem. Soc.* **2018**, *140*, 14511−14525.

(8) Vogler, A.; Kunkely, H. Ligand-to-ligand and intraligand charge transfer and their relation to charge transfer interactions in organic zwitterions. *Coord. Chem. Rev.* **2007**, *251*, 577−583.

(9) (a) Haskel, A.; Straub, T.; Eisen, M. S. Organoactinide-Catalyzed Intermolecular Hydroamination of Terminal Alkynes. *Organometallics* **1996**, *15*, 3773−3775. (b) Garner, M. E.; Hohloch, S.; Maron, L.; Arnold, J. A New Supporting Ligand in Actinide Chemistry Leads to Reactive Bis(NHC)borate-Supported Thorium Complexes. *Organometallics* **2016**, *35*, 2915−2922. (c) Bell, N. L.; Maron, L.; Arnold, P. L. Thorium Mono- and Bis(imido) Complexes Made by Reprotonation of cyclo-Metalated Amides. *J. Am. Chem. Soc.* **2015**, *137*, 10492−10495. (d) Vilanova, S. P.; del Rosal, I.; Tarlton, M. L.; Maron, L.; Walensky, J. R. Functionalization of Carbon Monoxide and tert-Butyl Nitrile by Intramolecular Proton Transfer in a Bis(Phosphido) Thorium Complex. *Angew. Chem., Int. Ed.* **2018**, *57*, 16748−16753. (e) Ren, W.; Zi, G.; Fang, D.-C.; Walter, M. D. A Base-Free Thorium−Terminal-Imido Metallocene: Synthesis, Structure, and Reactivity. *Chem. - Eur. J.* **2011**, *17*, 12669−12682. (f) Ren, W.; Zi, G.; Walter, M. D. Synthesis, Structure, and Reactivity of a Thorium Metallocene Containing a 2,2′-Bipyridyl Ligand. *Organometallics* **2012**, *31*, 672−679. (g) Yang, P.; Zhou, E.; Hou, G.; Zi, G.; Ding, W.; Walter, M. D. Experimental and Computational Studies on the Formation of Thorium−Copper Heterobimetallics. *Chem. - Eur. J.* **2016**, *22*, 13845−13849. (h) Zhang, C.; Yang, P.; Zhou, E.; Deng, X.; Zi, G.; Walter, M. D. Reactivity of a Lewis Base Supported Thorium Terminal Imido Metallocene toward Small Organic Molecules. *Organometallics* **2017**, *36*, 4525−4538. (i) Zhang, C.; Hou, G.; Zi, G.; Ding, W.; Walter, M. D. An Alkali-Metal Halide-Bridged Actinide Phosphinidiide Complex. *Inorg. Chem.* **2019**, *58*, 1571−1590.

(10) Shannon, R. D. Revised effective ionic radii and systematic studies of interatomic distances in halides and chalcogenides. *Acta Crystallogr., Sect. A: Cryst. Phys., Diffr., Theor. Gen. Crystallogr.* **1976**, *32*, 751−767.

(11) Glendening, E. D.; Badenhoop, J. K.; Reed, A. E.; Carpenter, J. E.; Bohmann, J. A.; Morales, C. M.; Weinhold, F. *NBO* 6.0; University of Wisconsin, Madison, WI, 2001.

(12) (a) Kelley, M. P.; Deblonde, G. J. P.; Su, J.; Booth, C. H.; Abergel, R. J.; Batista, E. R.; Yang, P. Bond Covalency and Oxidation State of Actinide Ions Complexed with Therapeutic Chelating Agent

DOI: 10.1021/jacs.9b04061
J. Am. Chem. Soc. XXXX, XXX, XXX−XXX

3,4,3-LI(1,2-HOPO). *Inorg. Chem.* **2018**, *57*, 5352−5363. (b) Su, J.; Batista, E. R.; Boland, K. S.; Bone, S. E.; Bradley, J. A.; Cary, S. K.; Clark, D. L.; Conradson, S. D.; Ditter, A. S.; Kaltsoyannis, N.; Keith, J. M.; Kerridge, A.; Kozimor, S. A.; Löble, M. W.; Martin, R. L.; Minasian, S. G.; Mocko, V.; La Pierre, H. S.; Seidler, G. T.; Shuh, D. K.; Wilkerson, M. P.; Wolfsberg, L. E.; Yang, P. Energy-Degeneracy-Driven Covalency in Actinide Bonding. *J. Am. Chem. Soc.* **2018**, *140*, 17977−17984. (c) Kaltsoyannis, N. Does Covalency Increase or Decrease across the Actinide Series? Implications for Minor Actinide Partitioning. *Inorg. Chem.* **2013**, *52*, 3407−3413. (d) Wilson, R. E.; De Sio, S.; Vallet, V. Protactinium and the intersection of actinide and transition metal chemistry. *Nat. Commun.* **2018**, *9*, 622.

(13) Fraser, R. R.; Mansour, T. S.; Savard, S. Acidity measurements on pyridines in tetrahydrofuran using lithiated silylamines. *J. Org. Chem.* **1985**, *50*, 3232−3234.

(14) Eppinger, J.; Herdtweck, E.; Anwander, R. Synthesis and characterization of alkali metal bis(dimethylsilyl) amides: infinite all-planar laddering in the unsolvated sodium derivative. *Polyhedron* **1998**, *17*, 1195−1201.

(15) Grant, L. N.; Pinter, B.; Gu, J.; Mindiola, D. J. Molecular Zirconium Nitride Super Base from a Mononuclear Parent Imide. *J. Am. Chem. Soc.* **2018**, *140*, 17399−17403.

(16) Warren, J. J.; Tronic, T. A.; Mayer, J. M. Thermochemistry of Proton-Coupled Electron Transfer Reagents and its Implications. *Chem. Rev.* **2010**, *110*, 6961−7001.

(17) Bogart, J. A.; Lippincott, C. A.; Carroll, P. J.; Booth, C. H.; Schelter, E. J. Controlled Redox Chemistry at Cerium within a Tripodal Nitroxide Ligand Framework. *Chem. - Eur. J.* **2015**, *21*, 17850−17859.

(18) Iluc, V. M.; Miller, A. J. M.; Anderson, J. S.; Monreal, M. J.; Mehn, M. P.; Hillhouse, G. L. Synthesis and Characterization of Three-Coordinate Ni(III)-Imide Complexes. *J. Am. Chem. Soc.* **2011**, *133*, 13055−13063.

(19) (a) Evans, W. J. The expansion of divalent organolanthanide reduction chemistry via new molecular divalent complexes and sterically induced reduction reactivity of trivalent complexes. *J. Organomet. Chem.* **2002**, *647*, 2−11. (b) Arnold, P. L.; Patel, D.; Wilson, C.; Love, J. B. Reduction and selective oxo group silylation of the uranyl dication. *Nature* **2008**, *451*, 315. (c) Arnold, P. L.; Pécharman, A.-F.; Lord, R. M.; Jones, G. M.; Hollis, E.; Nichol, G. S.; Maron, L.; Fang, J.; Davin, T.; Love, J. B. Control of Oxo-Group Functionalization and Reduction of the Uranyl Ion. *Inorg. Chem.* **2015**, *54*, 3702−3710.

DOI: 10.1021/jacs.9b04061
J. Am. Chem. Soc. XXXX, XXX, XXX−XXX